A Micro-turbine Model for System Studies Incorporating Validated Thermodynamic Data

G. J. Kish, *Member, IEEE,* and P. W. Lehn, *Senior Member, IEEE*

***Abstract*—There is an apparent lack of micro-turbine dynamic models available in literature that include valid experimental data. In an effort to help fill this gap a thermodynamic based micro-turbine model supplemented with experimental data & validated calculations is introduced. The data was extracted from a study on the 60 kW Capstone C60 MicroTurbine^{TM}. Transfer functions describing the micro-turbine model valid for various types of studies are defined; namely EMTP studies, controller design, small signal and stability analyses. Simulations are performed in PSCAD/EMTDC to validate the derived transfer functions, and to investigate the micro-turbine transient response. Researchers can utilise this calibrated model within their power system studies to quantify the application of micro-turbines as distributed generating sources within the distribution network.**

***Index Terms*—Distributed power generation, dynamics, micro-turbine, PSCAD, thermodynamics.**

I. Introduction

DUE to numerous driving factors the penetration of distributed generation (DG) within the distribution network has been steadily increasing in recent years. Depending on the application there are various DG technologies that utilities and industry can select from for inclusion into their power generation projects. Some specific technologies include photo-voltaic, wind, biomass, micro-turbines and fuel cells. Of these, micro-turbines have garnered attention lately as a promising DG technology because of their [1] (i) ability to provide baseload generation, load-shedding and peak-shaving functionalities, (ii) ability to operate for extended periods with minimal maintenance, (iii) small size relative to other DG, (iv) flexibility in using various commercially available fuel types, (v) low NO_X emissions, and (vi) increased energy efficiency when functioning as a combined heat and power (CHP) system. They are also well suited for remote electrification projects or micro-grid applications.

Because of its rising popularity as a DG candidate the simulation of micro-turbine based power generation systems is an active research area. Researchers are performing numerous studies to investigate the response characteristics of micro-turbines. Such studies include micro-turbines in grid-connected and stand-alone configurations, load-following applications and transient stability analysis. To accommodate these system studies there is an obvious desire for dynamic models to closely reflect the actual micro-turbine operation; ideally the model should contain accurate data. However, a lack of simple dynamic models with experimental data valid for micro-turbines has been noted in the literature.

The authors are with the Department of Electrical and Computer Engineering, University of Toronto, Toronto, ON M5S 3G4 Canada.

978-1-4577-1002-5/11/$26.00

The majority of models presently being used for dynamic analyses of micro-turbines were originally developed for much larger capacity gas-turbines on the scale of megawatts (i.e, 18 MW to 106 MW [2]). In comparison, micro-turbines are designed for capacities in the range of 25 to 300 kW [1].

A significant number of publications utilise the two following dynamic models: (i) the heavy-duty gas-turbine model developed by W. I. Rowen [2] at GE in 1983, which has been used by several authors [3]–[9] (commonly supplemented with the data from [10]), and (ii) the Western System Coordinating Council (WSCC) compliant GAST model, which has been employed by [11]–[14]. Although other models exist in literature [15]–[18] the Rowen and GAST models are the most prevalent. Both of these models were developed based on large capacity gas-turbines normally situated in central power generating plants.

The experimental data in the Rowen and GAST models consist of fuel system dynamics, compartment temperatures, speed-governor coefficients and rotor inertias. In many cases this data is being directly applied to the modelling of micro-turbines with little or no modification [7]. As such it is reasonable to infer any time constants would not accurately represent the response characteristics of modern micro-turbine designs. Moreover, it is unlikely that micro-turbine compartment temperatures or governor controls would remain identical to their gas-turbine counterparts, which in the case of the Rowen model are over 25 years old. To aid researchers in performing system studies of micro-turbines it would be highly beneficial to provide a dynamic model that could better characterise their performance.

In this paper a micro-turbine thermodynamic model is presented that incorporates experimental data & validated calculations based on a study of the 60 kW Capstone C60 MicroTurbine^{TM} by [19]. This data is used to calibrate the micro-turbine model of [20], which was adapted from [21] for micro-turbine applications. The C60 MicroTurbine^{TM} [22] was chosen as it is an established model available from Capstone, a prominent commercial micro-turbine manufacturer. By merging the separate works of [19] and [20] a calibrated model is provided to researchers for adoption into their power system dynamic studies of micro-turbines, to be used for further evaluation.

The model provides a mechanical shaft power output for input to a high-speed permanent magnet synchronous generator (PMSG). Because the focus of this work pertains to a thermodynamic micro-turbine model for inclusion into a micro-turbine based generation system, the PMSG and grid-interfacing power electronics are not represented. Transfer functions of varying complexity are derived from the model to give insight into the micro-turbine's dynamic response. The model is implemented in the PSCAD/EMTDC simulation environment to validate the transfer functions and evaluate the micro-turbine's response when subjected to transients.

II. Thermodynamic Model Equations

This section briefly highlights the algebraic & differential equations for each of the three thermodynamic compartments of the micro-turbine: (i) compressor, (ii) combustion chamber and (iii) turbine. These equations are based on the initial work by [20], [23]. However, some modifications have been made to more accurately quantify the thermodynamic process within certain compartments; these changes will be explicitly noted. In [21] a detailed description of the thermodynamic process within each compartment can be found, along with derivations for the governing equations.

For clarity all variables will have their time dependence explicitly stated when they are first presented as some of the proceeding formulae include time delays. This time dependence will be dropped in subsequent sections.

A. Compressor

The relationship between air mass flow rates at the compressor inlet and outlet ports is

$$\dot{m}_{\mathrm{c}}(t) = \dot{m}_{\mathrm{a}}(t - \tau_{\mathrm{c}}). \tag{1}$$

Here $\dot{m}_{\mathrm{c}}(t)$ is the compressor outlet air mass flow rate, $\dot{m}_{\mathrm{a}}(t)$ is the inlet air mass flow rate, and τ_{c} is the compressor time constant which is equal to the ratio of compressor compartment length to the mean air speed through the compartment.

The thermal power required to pressurize the inlet air is

$$P_{\mathrm{thc}}(t) = 0.5\overline{Cp}_{\mathrm{air}}[\dot{m}_{\mathrm{a}}(t) + \dot{m}_{\mathrm{c}}(t)][T_{\mathrm{c}}(t) - T_{\mathrm{a}}(t)], \tag{2}$$

where $P_{\mathrm{thc}}(t)$ is the thermal power consumed by the compressor, $T_{\mathrm{c}}(t)$ is the compressor outlet temperature, $T_{\mathrm{a}}(t)$ is the inlet air ambient temperature, and $\overline{Cp}_{\mathrm{air}}$ is the average specific heat capacity of the inlet air between $T_{\mathrm{a}}(t)$ and $T_{\mathrm{c}}(t)$.

The specific heat capacity is not constant between state points on the micro-turbine cycle temperature-entropy diagram, but rather a function of temperature (i.e., $Cp_{\mathrm{air}} = Cp_{\mathrm{air}}(T)$), and hence $\overline{Cp}_{\mathrm{air}}$ is used to increase the accuracy in calculating $P_{\mathrm{thc}}(t)$ [19]. This is in contrast to the thermal power calculations in [20] and [21], which both assume the inlet air specific heat capacity is constant regardless of temperature variation. When considering large temperature differentials this can introduce significant calculation errors.

The mechanical power consumed by the compressor, $P_{\mathrm{c}}(t)$, is related to the compressor's thermal power consumption by

$$\tau_{\mathrm{c}}\frac{\mathrm{d}}{\mathrm{d}t}P_{\mathrm{c}}(t) = P_{\mathrm{thc}}(t) - P_{\mathrm{c}}(t). \tag{3}$$

B. Combustion Chamber

The amount of fuel injected into the combustion chamber is in proportion to $\dot{m}_{\mathrm{a}}(t)$

$$\dot{m}_{\mathrm{f}}(t) = k_{\mathrm{afr}}^{-1}\dot{m}_{\mathrm{a}}(t). \tag{4}$$

Here $\dot{m}_{\mathrm{f}}(t)$ is the mass flow rate of the fuel, and k_{afr} is the inlet air to fuel ratio. The fuel considered in this work is natural gas, which is a commonly utilised energy source for the Capstone C60 MicroTurbine^{TM} unit.

The mass flow rate at the combustion chamber outlet port is characterised by

$$\dot{m_{\mathrm{cc}}}(t) = \dot{m}_{\mathrm{c}}(t - \tau_{\mathrm{cc}}) + \dot{m}_{\mathrm{f}}(t - \tau_{\mathrm{cc}}), \tag{5}$$

where $\dot{m_{\mathrm{cc}}}(t)$ is the mass flow rate of the exhaust gas exiting the combustion chamber, and τ_{cc} is the combustion chamber time constant which is equal to the ratio of combustion chamber compartment length to the mean air speed through the compartment.

It should be noted that the combustion process does not directly generate mechanical power output; it increases the energy content of the gas passing through it.

C. Turbine

The air mass flow rate at the turbine outlet is given by

$$\dot{m}_{\mathrm{t}}(t) = \dot{m_{\mathrm{cc}}}(t - \tau_{\mathrm{t}}). \tag{6}$$

$\dot{m}_{\mathrm{t}}(t)$ is the turbine air mass flow rate, and τ_{t} is the turbine time constant which is equal to the ratio of turbine compartment length to the mean air speed through the compartment.

The thermal power generated by the turbine is

$$P_{\mathrm{tht}}(t) = 0.5\overline{Cp}_{\mathrm{exh}}[\dot{m}_{\mathrm{t}}(t) + \dot{m_{\mathrm{cc}}}(t)][T_{\mathrm{cc}}(t) - T_{\mathrm{t}}(t)]. \tag{7}$$

Here $P_{\mathrm{tht}}(t)$ is the thermal power generated by the turbine, $T_{\mathrm{cc}}(t)$ is the combustion chamber outlet temperature, $T_{\mathrm{t}}(t)$ is the turbine outlet temperature, and $\overline{Cp}_{\mathrm{exh}}$ is the average specific heat capacity of the exhaust gas between $T_{\mathrm{t}}(t)$ and $T_{\mathrm{cc}}(t)$.

Similar to the discussion regarding $\overline{Cp}_{\mathrm{air}}$ within (2), $\overline{Cp}_{\mathrm{exh}}$ accounts for the temperature dependence of the specific heat capacity. This becomes increasingly important here for reducing calculation errors as this compartment typically experiences relatively high temperature drops. Moreover, a subtle point to note is the specific heat capacities in (2) and (7) are different quantities. Compared to the strategy employed by [20] and [21] where the specific heat capacities of the inlet air and exhaust gas were assumed equal, this more accurately reflects the thermodynamic process within each compartment.

The turbine generates a mechanical power output, $P_{\mathrm{t}}(t)$, which is governed by

$$\tau_{\mathrm{t}}\frac{\mathrm{d}}{\mathrm{d}t}P_{\mathrm{t}}(t) = P_{\mathrm{tht}}(t) - P_{\mathrm{t}}(t). \tag{8}$$

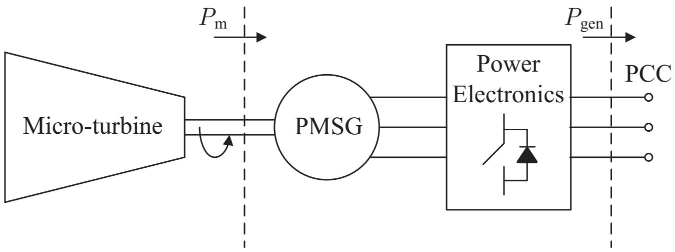

Fig. 1. Simplified component diagram for the Capstone C60 MicroTurbine^{TM}.

TABLE I
MODEL PARAMETERS FOR 100% LOADING

Parameter at 100% loading	Value
Compressor time constant, τ_c [ms]	1.3
Combustion chamber time constant, τ_{cc} [ms]	1.4
Turbine time constant, τ_t [ms]	0.3
Inlet air ambient temperature, T_a [°C]	28.6
Compressor outlet temperature, T_c [°C]	201.9
Combustion chamber outlet temperature, T_{cc} [°C]	922.9
Turbine outlet temperature, T_t [°C]	634.9
Inlet air average specific heat capacity, $\overline{Cp}_{air}$ [J/Kg °C]	1016
Exhaust gas average specific heat capacity, $\overline{Cp}_{exh}$ [J/Kg °C]	1188
Inlet air to fuel (natural gas) ratio, k_{afr}	93.1

III. MICRO-TURBINE MODEL

The net mechanical power output generated by the micro-turbine, $P_m(t)$, is the difference between the mechanical power generated by the turbine and the mechanical power consumed by the compressor

$$P_m(t) = P_t(t) - P_c(t). \tag{9}$$

This power output from the micro-turbine is the power exerted on the turbine shaft. For the Capstone C60 MicroTurbine^{TM} the turbine shaft is directly coupled to a high-speed PMSG. To calculate the net electrical power at the output terminals of the micro-turbine generation system, $P_{gen}(t)$, the following is considered [19]

$$P_{gen}(t) = P_m(t)\eta_{mech}\eta_{pmsg}\eta_{elec}, \tag{10}$$

where η_{mech} is the mechanical efficiency of the system (e.g., shaft/bearing losses, turbine damping, etc.), η_{pmsg} is the PMSG efficiency and η_{elec} is the electrical efficiency of the grid-interfacing power electronics. Fig. 1 shows a simplified diagram of the Capstone C60 MicroTurbine^{TM} system components. Here P_{gen} is defined as the power injected at the point of common coupling (PCC). Although this paper does not directly address the PMSG and power electronics, (10) is used in the subsequent section to justify the steady-state values of $P_m(t)$.

After applying the Laplace operator to (1) through (9) a block diagram for the micro-turbine thermodynamic model can be formed as depicted in Fig. 2. The input and output of the model is $\dot{m}_a$ and P_m, respectively. This implies the micro-turbine's output power is controlled by adjusting the inlet air mass flow rate.

IV. VALIDATED MODEL DATA

In [19] an extensive energy and exergy study was performed on a Capstone C60 MicroTurbine^{TM} installation [24] at the central utility plant on the Mississauga campus at the University of Toronto. While in the grid-connected operating mode, experimental data was collected from the micro-turbine corresponding to three different loading conditions: (i) 100%, (ii) 75%, and (iii) 50%. Data measurements for each steady-state loading condition were recorded every few minutes, over the course of several hours.

A complete model of all the micro-turbine compartments was formulated in [19] based on the first and second law of thermodynamics, and using MATLAB this model was used to generate predicted results at each of the three loading conditions. These predicted results showed good agreement with the experimental data collected across all the micro-turbine's loading points, thereby validating the model. The predicted results consist of various thermodynamic properties of the inlet air and exhaust gas at different states on a temperature-entropy diagram of the micro-turbine cycle.

The thermodynamic parameters of the Capstone C60 MicroTurbine^{TM} relevant to the model in Fig. 2 were extracted from the experimental data & validated results in [19]. Model parameters associated with 100%, 75% and 50% loading of the micro-turbine are listed in Table I, Table II and Table III, respectively. The only exception are the compressor, combustion chamber and turbine time constants; these values were retained from [20].

The time constants are relatively fast as they are on the order of a couple ms. The physical reason is due to the small compartment sizes and relatively fast gas speeds within the micro-turbine [20]. This is in stark contrast to the fuel system dynamics for the Rowen model available in [10], which have time constants on the order of hundreds of ms.

Using the data in Tables I through III the steady-state mechanical power values in Fig. 2 were calculated. They are summarised in Table IV. Note that the power consumed by the compressor compartment is nearly equal to the mechanical power output of the micro-turbine. This power ratio is very similar to a reference gas-turbine cycle in a study performed by [25] where P_t, P_c and P_m are 447 kW, 222 kW and 225 kW, respectively. This correlation affirms the values in Table IV are indeed practical.

The values for P_m in Table IV are considerably larger then the designed values of P_{gen}; 60 kW at 100% loading, 45 kW at 75% loading and 30 kW at 50% loading. As Fig. 1 and (10) illustrate this is due to losses for system components external to the micro-turbine model. In [19] the experimental data included measured values for η_{elec} of 0.945, 0.917 and 0.893 at 100%, 75% and 50% loading, respectively. Using (10) this gives realistic values for $(\eta_{mech}\eta_{pmsg})$ of 0.906, 0.905 and 0.896, respectively.

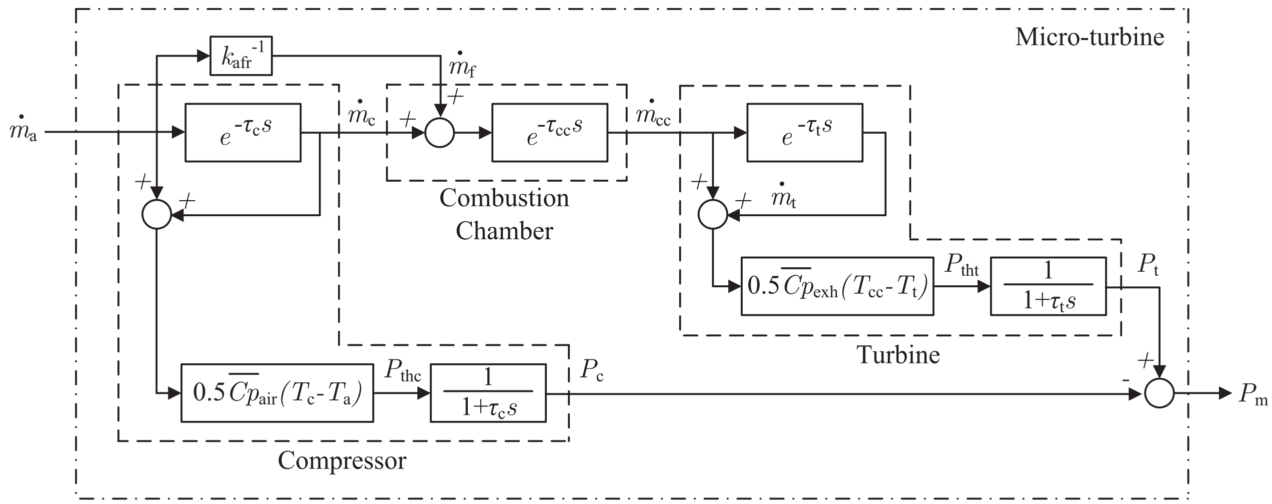

Fig. 2. Micro-turbine thermodynamic model.

TABLE II
MODEL PARAMETERS FOR 75% LOADING

Parameter at 75% loading	Value
Compressor time constant, τ_{c} [ms]	1.3
Combustion chamber time constant, τ_{cc} [ms]	1.4
Turbine time constant, τ_{t} [ms]	0.3
Inlet air ambient temperature, T_{a} [°C]	28.7
Compressor outlet temperature, T_{c} [°C]	180.9
Combustion chamber outlet temperature, T_{cc} [°C]	893.9
Turbine outlet temperature, T_{t} [°C]	634.9
Inlet air average specific heat capacity, $\overline{Cp}_{\mathrm{air}}$ [J/K$_{\mathrm{g}}$ °C]	1017
Exhaust gas average specific heat capacity, $\overline{Cp}_{\mathrm{exh}}$ [J/K$_{\mathrm{g}}$ °C]	1179
Inlet air to fuel (natural gas) ratio, k_{afr}	103.7

TABLE III
MODEL PARAMETERS FOR 50% LOADING

Parameter at 50% loading	Value
Compressor time constant, τ_{c} [ms]	1.3
Combustion chamber time constant, τ_{cc} [ms]	1.4
Turbine time constant, τ_{t} [ms]	0.3
Inlet air ambient temperature, T_{a} [°C]	28.8
Compressor outlet temperature, T_{c} [°C]	153.9
Combustion chamber outlet temperature, T_{cc} [°C]	850.9
Turbine outlet temperature, T_{t} [°C]	634.7
Inlet air average specific heat capacity, $\overline{Cp}_{\mathrm{air}}$ [J/K$_{\mathrm{g}}$ °C]	1014
Exhaust gas average specific heat capacity, $\overline{Cp}_{\mathrm{exh}}$ [J/K$_{\mathrm{g}}$ °C]	1165
Inlet air to fuel (natural gas) ratio, k_{afr}	118.3

TABLE IV
MICRO-TURBINE STEADY-STATE POWER VALUES

Power	Micro-turbine loading		
	100%	75%	50%
P_{t} [kW]	142.9	108.8	74.9
P_{c} [kW]	72.8	54.6	37.4
P_{m} [kW]	70.1	54.2	37.5

V. SIMULATIONS AND RESULTS

This section investigates the dynamic output response of the micro-turbine model in Fig. 2 with the 100% loading parameters of Table I. The model was implemented in the PSCAD/EMTDC simulation environment. Simulations for the cases of 75% and 50% micro-turbine loading are not shown as they exhibit the same general response characteristics for the 100% loading condition, but with different steady-state values.

To perform a transient analysis of the micro-turbine at each steady-state loading point it is assumed the temperatures change slowly with respect to the compressor, combustion chamber and turbine time constants; and thus they can be held constant during the simulations.

A. Open-Loop Response

The open loop response of P_{m} to a step change in $\dot{m}_{\mathrm{a}}$, corresponding to a change in P_{m} from 0.8 to 1.0 per-unit, is shown in Fig. 3. Note the non-minimum phase response of the output power. It is quite substantial and corresponds to an initial 10.8 kW drop in output power. This occurs because with the step change in air flow, mechanical power is first taken from the turbine shaft to compress the required air. After a short amount of time the mechanical power generated by the turbine compensates for this initial reduction in shaft kinetic energy [21].

The dynamic response of the micro-turbine is fairly quick as the output power settles in about 10ms. This fast response is manifested by the small time constants in Tables I through III.

B. System Transfer Function

To gain insight into the dynamics of the micro-turbine a transfer function representation of the system is required. The first-order lag approximation [26]

$$e^{-\tau s} \approx \frac{1}{1+s\tau} \tag{11}$$

was applied to each of the exponential terms in Fig. 2. Each first-order lag term is valid for a phase contribution up to 57°. For the system in Fig. 2 this gives ample phase representation. This leads to the approximated system transfer function

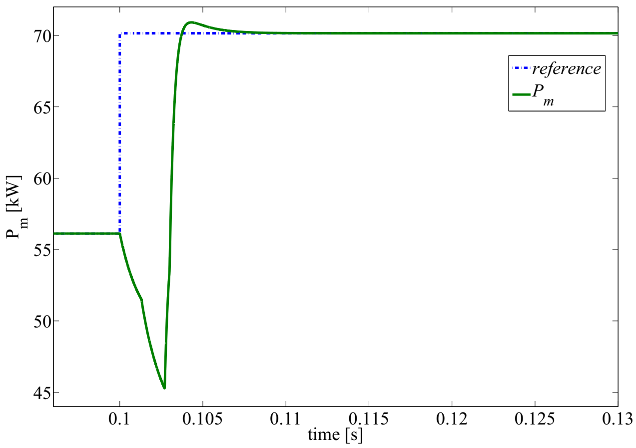

Fig. 3. Micro-turbine output power open loop step response.

$$\frac{P_{\mathrm{m}}(s)}{\dot{m}_{\mathrm{a}}(s)} \approx M(s) = \frac{k_{\mathrm{e}}\sigma_{t2}\sigma_{c1}(1 + k_{\mathrm{afr}}^{-1}\sigma_{c1}) - k_{\mathrm{a}}\sigma_{c2}\sigma_{t1}^2\sigma_{cc}}{\sigma_{c1}^2\sigma_{t1}^2\sigma_{cc}}, \tag{12}$$

where

$$k_e = 0.5\overline{Cp}_{\mathrm{exh}}(T_{\mathrm{cc}} - T_{\mathrm{t}}) \tag{13}$$
$$k_a = 0.5\overline{Cp}_{\mathrm{air}}(T_{\mathrm{c}} - T_{\mathrm{a}}) \tag{14}$$
$$\sigma_{c1} = 1 + \tau_{\mathrm{c}}s \tag{15}$$
$$\sigma_{c2} = 2 + \tau_{\mathrm{c}}s \tag{16}$$
$$\sigma_{t1} = 1 + \tau_{\mathrm{t}}s \tag{17}$$
$$\sigma_{t2} = 2 + \tau_{\mathrm{t}}s \tag{18}$$
$$\sigma_{cc} = 1 + \tau_{\mathrm{cc}}s. \tag{19}$$

Here $M(s)$ is of sufficient accuracy to facilitate small signal analysis of the micro-turbine and/or perform controller design. In particular it permits design of a controller using classical linear methods (e.g., root locus or frequency-response). This avoids a heuristic approach to tuning a controller for regulation of the micro-turbine's output power, as was used by [20].

For transient stability studies it is a reasonable approximation to discard the fastest system poles from the transfer function and keep only the slower (dominant) poles. This makes for a simpler model and ideally requires less information about the micro-turbine. As the time constant associated with the turbine compartment is significantly faster than both the combustion chamber or compressor dynamics, τ_{t} can be neglected

$$\widehat{M(s)} = \frac{2k_{\mathrm{e}}\sigma_{c1}(1 + k_{\mathrm{afr}}^{-1}\sigma_{c1}) - k_{\mathrm{a}}\sigma_{c2}\sigma_{cc}}{\sigma_{c1}^2\sigma_{cc}}. \tag{20}$$

Depending on the study objectives a system model can be utilised which possesses the required system complexity: (i) the full model of Fig. 2, (ii) the approx. transfer function $M(s)$, or (iii) the reduced approx. transfer function $\widehat{M(s)}$.

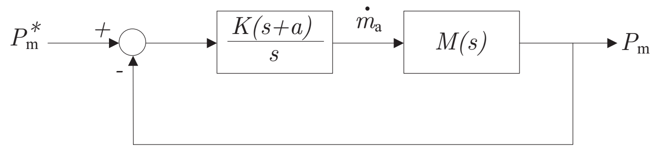

Fig. 4. Micro-turbine control system bock diagram.

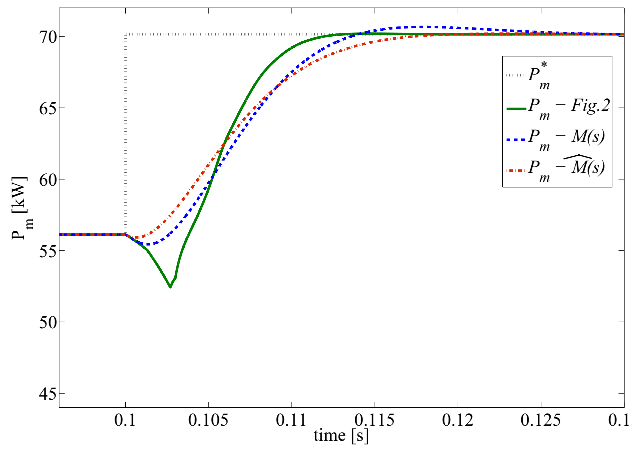

Fig. 5. Micro-turbine output power closed loop step response.

C. Closed-Loop Response

To regulate the micro-turbine's output power a simple PI compensator can be used as shown in Fig. 4. The compensator parameters K and a were determined as $7e^{-7}$ Kg/J and 1200 Kg/Js, respectively. Fig. 5 illustrates the closed loop response of P_{m} to a step change in P_{m}^* from 0.8 to 1.0 per-unit. The output P_{m} has been plotted for each of the models derived previously; Fig. 2, $M(s)$ and $\widehat{M(s)}$

In Fig. 5 the response curves arranged from quickest to longest settling times correspond to the full model of Fig. 2, $\widehat{M(s)}$ and $M(s)$, respectively. In addition, the only output response to exhibit a slight overshoot is the $M(s)$ model.

It is also observed that the closed-loop settling time, with respect to the full thermodynamic model of Fig. 2, has increased to 15ms from the open-loop (Fig. 3) value of 10ms. However, there is a significant improvement in the non-minimum phase response as the initial drop in output power is now only 3.7 kW.

VI. Conclusion

A thermodynamic based micro-turbine model incorporating experimental data and validated calculations from a 60 kW Capstone C60 MicroTurbine^{TM} has been presented. Three distinct sets of data have been provided which correspond to steady-state operating points for 100%, 75% and 50% micro-turbine loading. In addition to a complete thermodynamic model appropriate for EMTP type studies, two system transfer functions have been derived based on certain approximations and assumptions. The model $M(s)$, represented by (12), is sufficient for small signal analysis and controller design. The model $\widehat{M(s)}$, represented by (20), is valid for transient stability analyses.

Simulations have shown that the micro-turbine output power P_{m} exhibits a non-minimum phase response and has a relatively fast settling time due to the presence of small time constants. When contrasted against existing micro-turbine models that utilise data originally intended for large capacity gas-turbines, this model provides a more realistic representation of the micro-turbine for system studies. This will assist researchers in studying the application of micro-turbines as DG sources within the distribution network under different configurations or operating schemes, in an effort to quantify their impact on the power system.

References

[1] S. Chowdhury, S. P. Chowdhury and P. Crossley, *Microgrids and Active Distribution Networks*. Institution of Engineering and Technology (IET), 2009.

[2] W. Rowen, "Simplified mathematical representations of heavy duty gas turbines," *Transactions of the ASME. Journal of Engineering for Power*, vol. 105, no. 4, pp. 865 – 870, Oct 1983.

[3] D. N. Gaonkar, R. N. Patel, and G. N. Pillai, "Dynamic model of microturbine generation system for grid connected/islanding operation," in *IEEE International Conference on Industrial Technology, 2006. ICIT 2006.*, Dec 2006, pp. 305 – 310.

[4] D. N. Gaonkar and R. N. Patel, "Modeling and simulation of microturbine based distributed generation system," in *IEEE Power India Conference, 2006.*, 2006, pp. 256 – 260.

[5] S. R. Guda, C. Wang, and M. H. Nehrir, "Modeling of microturbine power generation systems," *Electric Power Components and Systems*, vol. 34, no. 9, pp. 1027 – 1041, Sep 2006.

[6] D. N. Gaonkar, G. N. Pillai, and R. N. Patel, "Seamless transfer of microturbine generation system operation between grid-connected and islanding modes," *Electric Power Components and Systems*, vol. 37, no. 2, pp. 174 – 188, Feb 2009.

[7] H. Wei, W. Ziping, N. Ming, Z. Jianhua, G. Yuanbo, and W. Chong, "Dynamic modelling and simulation of microturbine generation system for the parallel operation of microgrid," in *International Conference on Sustainable Power Generation and Supply, 2009. SUPERGEN '09.*, Apr 2009, pp. 1 – 8.

[8] M. Z. C. Wanik, and I. Erlich, "Simulation of microturbine generation system performance during grid faults under new grid code requirements," in *IEEE Bucharest PowerTech, 2009.*, Jun. 28 - Jul. 02 2009, pp. 1 – 8.

[9] G. Li, G. Li, W. Yue, M. Zhou, and K. L. Lo, "Modeling and simulation of a microturbine generation system based on PSCAD/EMTDC," in *5th International Conference on Critical Infrastructure (CRIS), 2010.*, Sep 2010, pp. 1 – 6.

[10] L. M. Hajagos and G. R. Bérubé, "Utility experience with gas turbine testing and modeling," in *IEEE Power Engineering Society Winter Meeting, 2001.*, vol. 2, 2001, pp. 671 – 677.

[11] Y. Zhu and K. Tomsovic, "Development of models for analyzing the load-following performance of microturbines and fuel cells," *Electric Power Systems Research*, vol. 62, no. 1, pp. 1 – 11, 2002.

[12] M. Y. El-Sharkh, N. S. Sisworahardjo, M. Uzunoglu, O. Onar, and M. S. Alam, "Dynamic behavior of PEM fuel cell and microturbine power plants," *Journal of Power Sources*, vol. 164, no. 1, pp. 315 – 321, 2007.

[13] A. K. Saha, S. Chowdhury, S. P. Chowdhury, and P. A. Crossley, "Modelling and simulation of microturbine in islanded and grid-connected mode as distributed energy resource," in *IEEE Power and Energy Society General Meeting - Conversion and Delivery of Electrical Energy in the 21st Century, 2008.*, Jul 2008, pp. 1 – 7.

[14] ——, "Modeling and performance analysis of a microturbine as a distributed energy resource," *IEEE Transactions on Energy Conversion*, vol. 24, no. 2, pp. 529 – 538, Jun 2009.

[15] R. Lasseter, "Dynamic models for micro-turbines and fuel cells," in *IEEE Power Engineering Society Summer Meeting, 2001.*, vol. 2, Jul 2001, pp. 761 – 766.

[16] S. Haugwitz, "Modelling of microturbine systems," in *European Control Conference ECC 2003*, 2003, pp. 1287 – 1292.

[17] O. Fethi, L.-A. Dessaint, and K. Al-Haddad, "Modeling and simulation of the electric part of a grid connected microturbine," in *IEEE Power Engineering Society General Meeting, 2004.*, vol. 2, Jun 2004, pp. 2212 – 2219.

[18] C. Boccaletti, S. Elia, and E. Nisticó, "A dynamical model of a gas microturbine generator for distributed generation," in *Proceedings of the 5th IASTED International Conference on Power and Energy Systems, EuroPES 2005.*, 2005, pp. 358 – 363.

[19] D. Yuan, "Energy and exergy evaluations on a microturbine system," Master's thesis, University of Toronto, 2007.

[20] H. Nikkhajoei, "Matrix converter and its application in a micro-turbine based generation system," Ph.D. dissertation, University of Toronto, 2004.

[21] H. -J. Nern, H. Kreshman, F. Fischer, and H. A. Nour Eldin, "Modelling of the long term dynamic performance of a gas turbo generator set," in *Proceedings of the Third IEEE Conference on Control Applications, 1994.*, vol. 1, Aug 1994, pp. 491 – 496.

[22] *Technical reference: Component Descriptions - Capstone model C60 MicroTurbine*$^{\mathrm{TM}}$, Capstone Turbine Corporation, Aug 2003, 410035-001 Rev B. [Online]. Available: http://www.capstoneturbine.com

[23] H. Nikkhajoei and R. Iravani, "Electromagnetic transients of a micro-turbine based distributed generation system," *Electric Power Systems Research*, vol. 77, no. 11, pp. 1475 – 1482, 2007.

[24] H. E. Jääskeläinen, and J. S. Wallace, "Operating experience with a 240 kw microturbine combined heating, cooling and power system," in *Proceedings of the 2nd International Conference on Energy Sustainability, 2008. ES 2008*, vol. 1, 2009, pp. 809 – 820.

[25] H. Kreshman, H. -J. Nern, and H. A. Nour Eldin, "Modelling and simulation of the dynamic behaviour of stationary gas turbine," in *Proceedings of the IMACS/IFAC International Symposium on Parallel and Distributed Computing in Engineering Systems, 1991.*, 1992, pp. 529 – 536.

[26] A. Buxbaum, K. Schierau and A. Straughen, *Design of Control Systems for DC Drives*, ser. EESES Electric Energy Systems and Engineering Series, J.G. Kassakian and D.H. Naunin, Ed. Springer-Verlag, 1990.

Gregory J. Kish (M'09) received the B.E.Sc. degree from the University of Western Ontario, London, ON, Canada in 2009 in electrical engineering, where he was a recipient of the Governor General's silver academic medal. He is currently a M.A.Sc student in electrical engineering at the University of Toronto, Toronto, ON.

Peter W. Lehn (SM'05) received the B.Sc. and M.Sc. degrees from the University of Manitoba, Winnipeg, MB, Canada in 1990 and 1992, respectively, both in electrical engineering. He received the Ph.D. degree in electrical engineering from the University of Toronto, Toronto, ON, Canada in 1999. From 1992 to 1994, he was with the Network Planning Group of Siemens AG, Erlangen, Germany. Currently, he is a Professor at the University of Toronto.